Numerical Simulation of High-Voltage Spacecraft Charging at High Altitudes: Comparison of NASCAP and ECO-M

V. V. Danilov, V.M. Dvoryashin, B.A. Elgin
Thermophysics Research Center, Krasnoyarsk State Technical University,
660074 Krasnoyarsk, Russia (e-mail: danilov@pine.krs.ru)
G. Drolshagen
ESA/ESTEC,NL-2200 AG Noordwijk, The Netherlands

Abstract

Computer simulation of spacecraft (SC) charging is one of the main means for the analysis of SC interaction with the hot plasma space environment. Results of two computer codes are presented: NASCAP and ECO-M. Both were applied to the simulation of high-voltage charging of a rotating SC. The analysed SC model is a conducting cylinder covered by thin dielectric material. The plasma environment, solar irradiation, secondary emission and other parameters correspond to realistic conditions for SC in geostationary orbit during a magnetic substorm. Two cases were analysed by both codes: 1) a continuously rotating cylinder; b) rotation starts after equilibrium charging was reached for a fixed orientation. In the first case the potential of illuminated SC surfaces increases steadily from 0 up to a steady-state level with oscillations resulting from the SC rotation frequency. In the second case a rapid potential jump after the beginning of rotation is observed. The potential of initially illuminated surface is changed from -3kV up to $+3$kV relative the space. A physical explanation of this effect is suggested. The main results of the computer simulations are: (a) a good agreement between ECO-M and NASCAP results, (b) SC rotation has a large influence on the high-voltage charging processes, (c) transition from eclipse to sunlight conditions could lead to sudden jumps of surface potentials.

1. INTRODUCTION

The modeling of spacecraft charging on computer is one of the main tools for the analysis of SC interaction with flows of hot plasma particles from space environment [1]. Since almost 20 years [2] the NASCAP code (NASA Charging Analyzer Program) is widely used in the US and Europe for numerical modeling of the processes of high-voltage charging. The ECO-M code (Electrization of Cosmic Objects) has been developed in Russia about a few years later [3]. ECO-M is applied, as NASCAP, to the analysis of charging processes for communication satellites at high altitudes. The algorithms of solving of a problem in ECO-M and NASCAP are quite different. A comparison of these two codes can show their strong and weak points and provide indications on the reliability of such numerical simulations.

2. COMPARISON OF ECO-M AND NASCAP CODES

Descriptions of NASCAP and ECO-M are given in [2, 3]. The main differences between the two codes are:

- The way the geometry is modelled. In NASCAP the object is formed on a 3-D cubic grid with dimensions $17 \times 17 \times 33$. A full spacecraft model typically consist of 1500 to a maximum 2000 surface cells. This is usually sufficient for the description of compact objects, but it is not possible to model more complex surfaces or extent objects which consist of several sub-moduls. In ECO-M the object description is based on the use of parameter sets of the surfaces. Such a geometry description gives a better accuracy for the analysis of real SC, because there is a strong dependence of field formation on the form of the surface. This permits to reproduce a configuration of various complexity including objects which are separated from each other in space. It is also possible to model, for example, the smooth rotation of solar arrays relatively to the SC body during its movement along the orbit.
- In NASCAP, for the calculation of fields and potentials in the vicinity of the object a method of final differences is used. As a result for each time step the distribution of potentials all around the object is determined. This algorithm permits to take into account the space charge near the object. On the other hand, however, for models with a complex relief of the surface it is difficult to determine the electric field strength directly on the surface of an object.

In ECO-M the calculation of potentials is based on a method of boundary integrated equations (BIE). Accordingly, at each step of iteration potentials as well as fields strength are defined directly on the surface of the object with an equal degree of accuracy. In conditions of high-voltage charging at high orbits when the Debye length of the plasma is large in comparison with the size of the SC such information in practice is fully sufficient. It also permits to separate the time consuming processing of the geometrical characteristics of a problem from the calculation charging dynamics. As a result CPU time is saved while still providing a high level of time resolution.

- The code algorithms related to the time resolution of the charging simulation are quite different. In ECO-M the program chooses a time step automatically according to a specified accuracy for the calculation of charging parameters. Usually this time step lies between 0.01s and 1s. Typical computing times in this case are 1-100s per step and ≈ 1000 steps are needed for a complete calculation. This permits to calculate the charging of objects for changing plasma environment parameters together with a detailed elaboration at a level of several seconds. Therefore, it is possible to consider dynamic effects like the variation of plasma parameters during a magnetic substorm as well as, for example, to simulate the passage of a SC through non-uniform plasma clouds, entry and exit from Earth's shadow of the Earth, and etc..

  In NASCAP the time step on time is usually chosen by the user (and automatic reduction or predefined step increase can be invoked as well). The user has to be very careful when selecting the time step. While the final equilibrium potentials are fairly independent of the time steps (provided the simulation is long enough) the temporal behavior of the charging process depends strongly (and often artificially) on the selected time step. NASCAP is based on a quasi-stationary approach and it is probably fair to say that NASCAP is not really suited to simulate highly dynamic plasma environments. NASCAP is usually installed on Work Station or larger computers, while ECO-M can comfortably run on PCs (Pentium).

At last, we shall note that the required set of surface material characteristics (conductivity, secondary emission and etc.) is comparable for both codes. But for the secondary emission, in addition to the maximum yield and corresponding energy, ECO-M uses a total yield value (integrated over energy) while NASCAP requires 4 parameters for yield curve. Both codes use Maxwellian distributions as standard for the description of plasma environment. The NASCAP calculations were conducted at ESA/ESTEC and the ECO-M simulation at Research Lab. "Cosmophysics" of Krasnoyarsk State University [4].

3. MODEL DESCRIPTION

For the comparison of NASCAP and ECO-M the following model and parameters set was chosen:
Spacecraft model: Cylinder: height 1 m, diameter 0.5 m. The Sun direction is normal to an axis of the cylinder (see fig.1b).

All external surfaces of the cylinder are covered by the same dielectric material. The following material characteristics were used:

- Thickness of the material: 0.1 mm.
- Photoelectron current for normally incident solar irradiation: $J_{photo} = 10^{-4}$ A/m^2 .
- Dielectric constant $\epsilon = 3$.
- Maximum value of secondary electron-electrons emission $\delta_{SEE} = 2.5$.
- Energy of electrons for maximum secondary e-e emission E = 0.3keV.
- Secondary ion - electrons emission $\delta_{SIE} = 0$.
- Bulk conductivity 10^{-15} Ohm^{-1}·m^{-1} .
- Surface resistance 10^{15} Ohm

Table 1. Steady-state potentials (in kV) for plate and cylinder.

Material	PLATE			Code
	sun	edge	shadow	
TRASH	−11.0	−21.3	−21.3	**NASCAP**
TRESH	−2.93	−5.66	−5.67	
TRASH	−9.97	−21.1	−21.1	**ECO-M**
TRESH	−3.16	−7.07	−7.07	

	CYLINDER - static			
	sun	basis	shadow	
TRESH	−3.02	−5.82	−5.82	**NASCAP**
TRESH	−3.44	−7.97	−7.97	**ECO-M**

The material with an electron-electrons emission $\delta_{SEE} = 2.5$ was denoted as TRESH. A second material, called TRASH, corresponds to an hypothetical material, for which only scattering of electrons is taken into account $\sigma = \eta$ ($\delta_{SEE} = 0$).

The plasma environment is described by an isotropic Maxwellian distribution function both for electrons and ions with equal temperatures ($n_e = n_i = 1$ cm^{-3}, $T_e = T_i = 10$ keV).

In combination with solar UV irradiation these parameters are not unrealistic for the conditions in geostationary orbit and real materials.

4. CYLINDER CHARGING

The following cases were analysed:

1. Static cylinder.

2. Continuously rotating cylinder (1 rpm around the Y axis Y which is the main the main long axis of the cylinder).

The numbering of surface elements for the NASCAP calculation is shown in Fig.1a.

4.1. Static cylinder

In Fig.2a,2b the results of the ECO-M and NASCAP calculations are shown. The levels of differential charging predicted by ECO-M are about 20% higher compared to the NASCAP values, but otherwise the charging behavior calculated by the two programs is in a good agreement. Table 1 gives a summary of equilibrium potentials predicted by ECO-M and NASCAP for the static cylinder as well as for a simple plate model. For the plate, materials with (TRESH) and without (TRASH) secondary emission were analysed.

4.2. Rotating cylinder

Inresting results were obtaind when the codes were applied to a rotating cylinder.

Changing sunlight exposure to a cylinder surface (here rotating with a period of 1 min) permits to reveal the main features of dynamic factors for spacecraft charging.

Fig.3a,b show the potential evolution for surface cell 110 located on the side of the cylinder (see Fig. 1a). For the NASCAP calculation the time step was selected as 7.5 s corresponding to 1/8 of a rotation. The potential oscillation on the cylinder side surface is a direct result of the periodic irradiation by the Sun. The potential at the shadowed cylinder basis monotonously decreases and reaches the same values as for the case of the static cylinder (see Fig.2b). The amplitude of the potential oscillations for illuminated surfaces lies within the limits of 60÷80V, and is similar for both codes.

We also study a variant in which the rotation of the cylinder was started after equilibrium charging levels had been reached. Such a situation could correspond, for example, to an attitude maneuver of the SC exposing charged surfaces to the Sun or to an eclipse to sunlight transition.

In Fig.5 the time evolutions of the potentials are plotted for the following cells: 110 (originally oriented to the Sun), and 78 (under an angle of 90^o to the Sun direction). As is apparent from the graphs, a strong change of potentials occurs for all surfaces, just after the onset of rotation. The most

Table 2. Potentials of elements of cylinder (kV). V_i — potential prior to the beginning of rotation, V_f — potential after beginning of rotation, $\Delta V = V_f - V_i$ — jump of potential after beginning of rotation.

Number of cells	110	78	23	61	**Code**
V_i	−3.00	−5.74	−5.74	−5.74	**NASCAP**
V_f	+1.02	+0.14	−0.07	−0.68	
ΔV	4.02	5.88	5.67	5.06	
V_i	−3.05	−6.23	−6.23	−6.23	**ECO-M** $\sigma_{total} = 0.9$
V_f	+3.30	+0.19	0	−0.23	
ΔV	6.35	6.42	6.23	6.00	
V_i	−5.80	−12.8	−12.8	−12.8	**ECO-M** $\sigma_{total} = 0.75$
V_f	+6.50	+0.02	+0.17	−0.24	
ΔV	12.3	12.8	13.0	12.6	

surprising result of these simulations is the occurrence of large positive potentials relative to space for some surface points. In Tab.2 data on potential values just before and after the start of the cylinder rotation are summarized. The maximum positive potential values are reached for cell 110 after the object has turned by 180^o.

For the ECO-M calculation the potential jump after start of rotation is about identical for all surfaces and amounts to 6.3±0.1 kV. For NASCAP the potential jumps by about 5.5± 0.4 kV except for the cell 110 for which it is only around 4 kV. The maximum level of differential charging obtained by ECO-M does practically not change after the beginning of rotation (from $\Delta V_i = 3.2$ kV to $\Delta V_f = 3.5$ kV).

For NASCAP with the beginning of rotation the differential charging changes from $\Delta V_i = 2.8$ kV to $\Delta V_f = 1.7$ kV.

The further evolution of the surface potentials after the initial jump consist of two stages: A first, fast phase, when the positive potentials on the surface disappear, and a second, slow phase, which is similar to the charging of a continuously rotating cylinder (see Fig.3). Both programs give similar time scale for the fast stage ≈ 200 s.

To better understand the observed potential jumps a second ECO-M calculation with a lower secondary emission yield of $\sigma_{total} = 0.75$ was performed. The results of this calculation are shown in Fig.6. The increase of the net electron current is resulting in an increase of the initial negative of potentials values on the object. Accordingly, the potential differences grow up to $\Delta V_i = 7$ kV. The potential jump of all points of the object in this case amounts to 12.3±0.8 kV. The time of the fast phase of the potential evolution after the start of rotation extends now up to ∼ 400s. The observed 60 s potential oscillations (the cycle period of rotation) have considerably large amplitude in this case.

6. DISCUSSION

For these phenomena which are occurring after the onset of rotation a simple physical explanation is suggested. The rates of charging of the object as a whole and its differential charging are considerably different for objects with thin dielectric covers. Therefore, when the rotation starts from steady-state stage of charging the differential potentials on the object persist for a relatively long time. When the cylinder is rotated by 180^o from an initial state the structure of the electric fields connected with differential charging does not suppress the photoemission current because of lack of a "saddle" type field structure. Therefore, the illuminated part of the object should acquire positive potential of the order of a few volts relative to space. The differential charging of the object will be conserved for some time. As a result, any fast (in comparison with characteristic times of differential charging) change of the potential of the illuminated SC part should be accompanied by a change of potentials for all points by the same amount as the potential jump for the illuminated part.

Consequently, according to this model the potential jump for cell 23 should be 5.8 kV and the potential value after half a rotation should be closed to zero. Accordingly, the expected potential of the cell 110 should be: V_f=-3kV+5.8kV=+2.8kV, when this cell has rotated to the shadowed back side.

ECO-M (see Tab.2) reproduces the potentials changes predicted by this model and also NASCAP gives qualitatively the same picture except the cell 110.

The proposed physical model also explains an increasing duration of the first ("fast") phase of the potential evolution (disappearance of positive potentials on the object) for decreasing secondary emission yields σ_{total}.

In fact, decreasing σ_{total} results in an increase of the amplitude of positive potentials (Fig.6). Discharging of the positively charged surfaces is done by the total current of electrons from the plasma because the secondary electron emission from the surface is blocked. Therefore, the duration of the fast discharging phase increases proportionally to the amplitude of the positive potential and does not depend on σ_{total}.

6. CONCLUSION

The comparison of ECO-M and NASCAP codes has shown good agreement in simulating high-voltage charging of a simple spacecraft model.

Two cases of rotating object were analysed: 1) a continuously rotating cylinder; b) rotation starts after equilibrium charging levels were reached for a fixed orientation. In the first case the negative potential of illuminated SC surfaces increases steadily from 0 up to an equilibrium level with oscillations resulting from the SC rotation frequency.

In the second case a rapid potential jump after the start of rotation is observed. The potential of initially illuminated surface changes from -3kV up to $+3$kV relative to space.

This effect can physically be explained by the much longer characteristic time for differential charging compared to absolute charging of the whole spacecraft.

Two main conclusions can be drawn from this study: 1. The results of these simulations should be considered for the interpretation of data for electron and ion distribution functions and other plasma parameters that are obtained by on board monitors.

2. Whenever a rapid temporal change of high-voltage surface potential could led to electrical discharges the analysis of dynamic high-voltage charging processes become very important for satellite designers .

It would be interesting to continue the comparison of ECO-M and NASCAP codes for more complicated SC models.

References

[1] Garrett H.B. The Charging of Spacecraft Surfaces, Rev. Geophys. Space Phys. Vol. 19,577,1981.

[2] Katz I., Cassidy J.J., Mandell M.J., Schneulle G.M., Steen P.G. and Roche J.C. "Capabilities of the NASA Charging Analyzer Program" Spacecraft Charging Technology. 1978. NASA CP-2071. AFGL TR-79-0082. 1979. P.101.

[3] Vasilyev Yu.V., Danilov V.V., Dvoryashin V.M., Kramarenko A.M. and Sokolov V.S. "Computer Modeling of Spacecraft Charging Using ECO-M", Proceedings of Int. Conf. Problems of Spacecraft / Environment Interaction, Novosibirsk, Russia. June 15-19.1992.P.203.

[4] Vasilyev Yu.V., Danilov V.V., Dvoryashin V.M., Kramarenko A.M. and Sokolov V.S."Comparison of ECO-M and NASCAP Codes for Modeling of High-Voltage Charging of Simple Test Objects" (in Russian) Preprint of Krasnoyarsk State University. N 2-93. 1993.

[5] Danilov V.V., Dvoryashin V.M., Kramarenko A.M., Sokolov V.S., Vasilyev Yu.V., Drolshagen G. and Leira P.P. "Numerical Simulation of High-Voltage Charging at High Altitudes; Comparison of NASCAP and ECO-M", ESA Symp.Proc. on "Environment Modeling for Space-based Application",ESTEC,Noordwijk,NL. September 18-20, pp.197-206.1996.

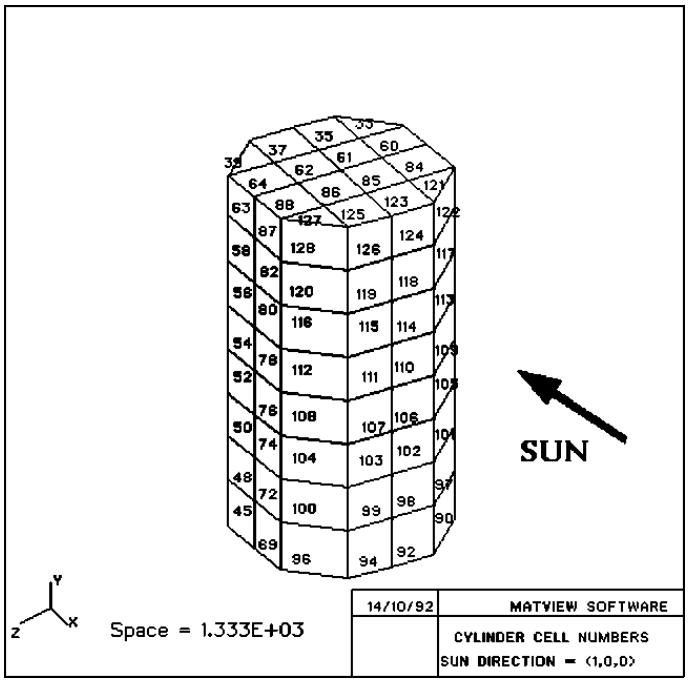

Fig.1a. Calculating model of cylinder (NASCAP presentation).

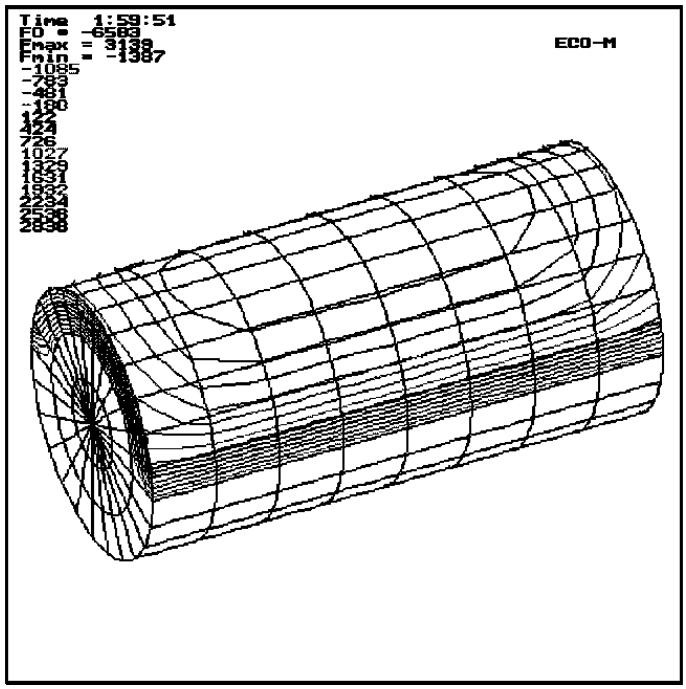

Fig.1b. ECO-M. Steady-state potential distribution on surface of static cylinder.

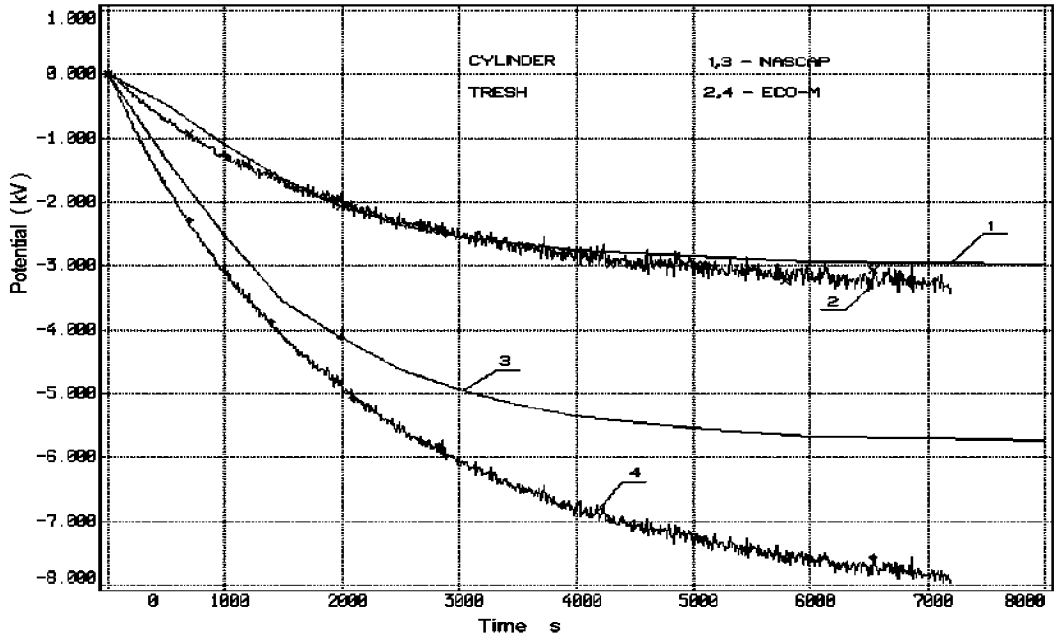

Fig.2a. Potential in center of illuminated (1,2) and shadowed (3,4) surfaces of static cylinder. 1,3 - NASCAP analysis, 2,4 - ECO-M analysis. TRESH material. Factor SEE at electron energy E=300 eV is δ_{max}= 2.5, σ_{total}=0.9.

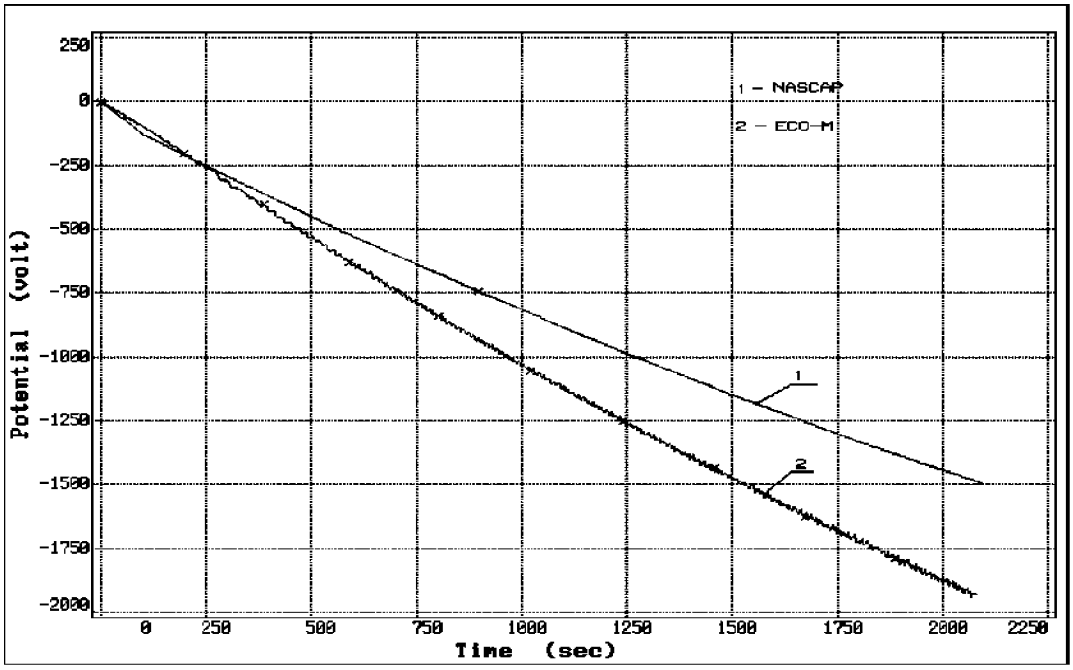

Fig.2b. Evolution of potential in center of rotating cylinder basis. 1 - NASCAP analysis, 2 - ECO-M analysis.

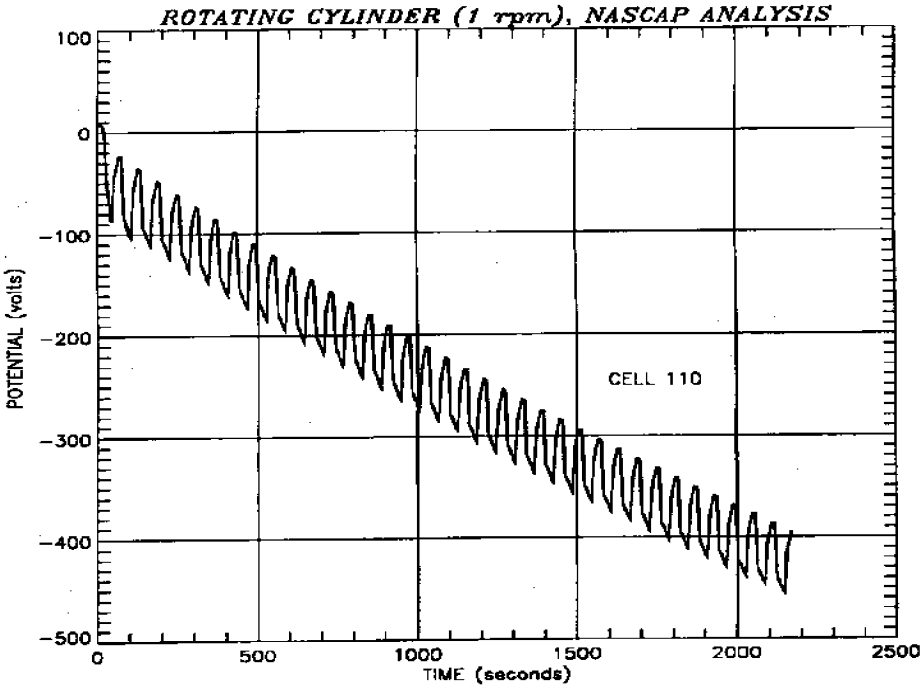

Fig.3a. NASCAP. Evolution of potential in center of lateral surface of rotating cylinder (ω =1 rpm).

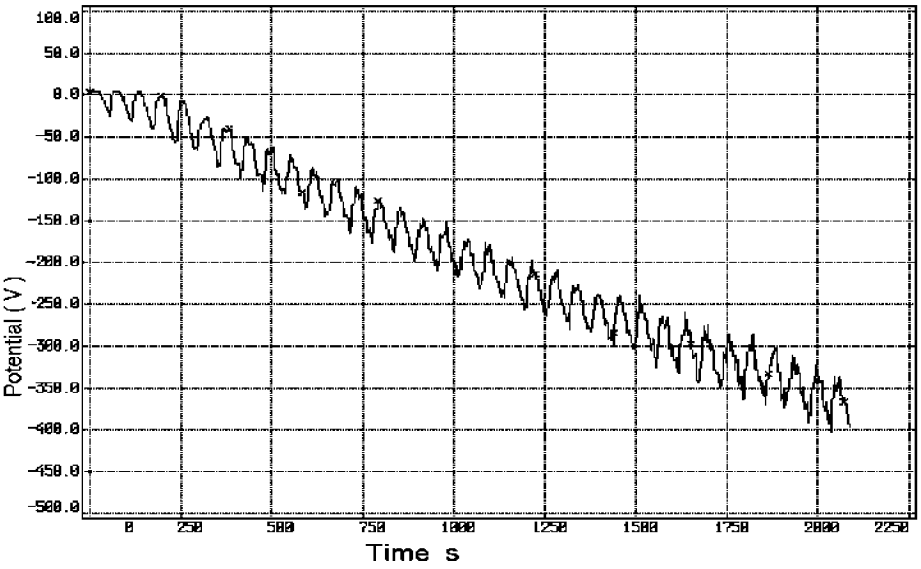

Fig.3b. ECO-M. Evolution of potential in center of lateral surface of rotating cylinder (ω =1rpm, σ_{total}=0.9).

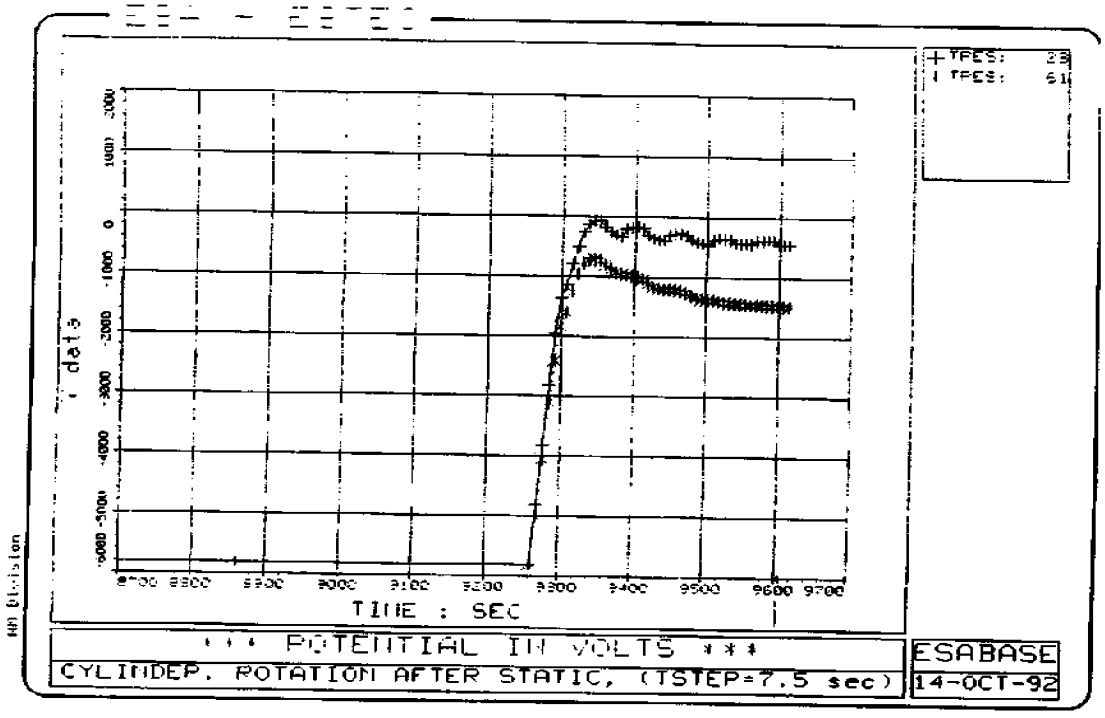

Fig.4a. NASCAP. Cylinder rotation after static charging. Start position of cell 23 is on shadowed surface, cell 61 is on cylinder basis.

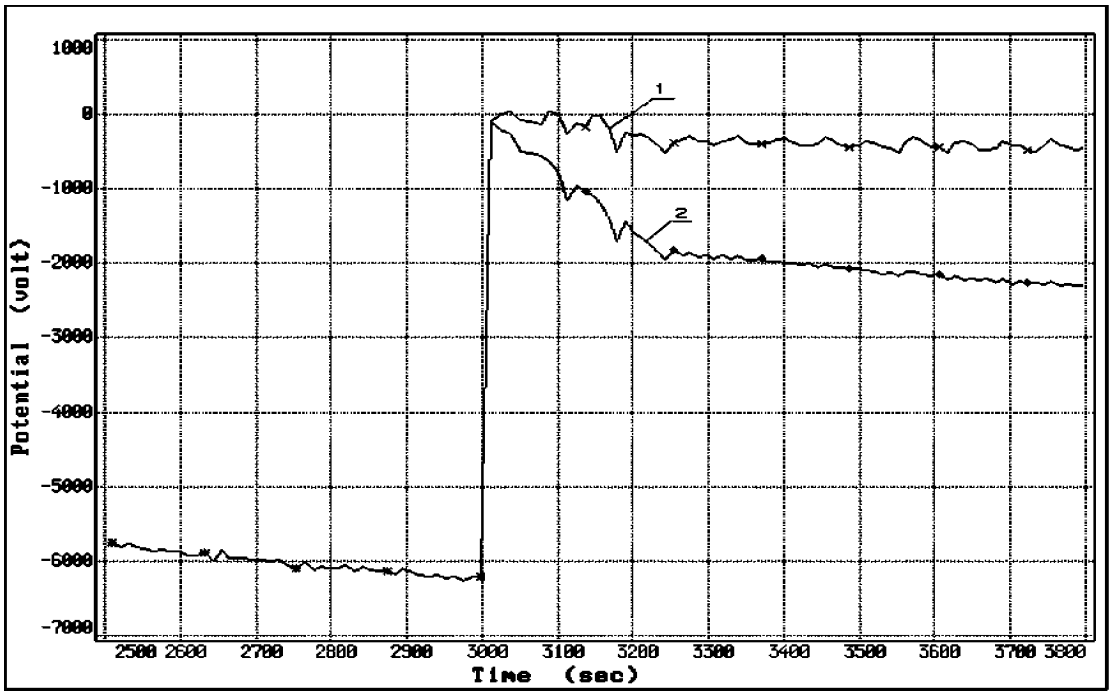

Fig.4b. ECO-M. Cylinder rotation after static charging (50 min after substorm begining). 1 - potential of lateral cylinder surface (cell 23), 2 - potential of cylinder basis (cell 61).

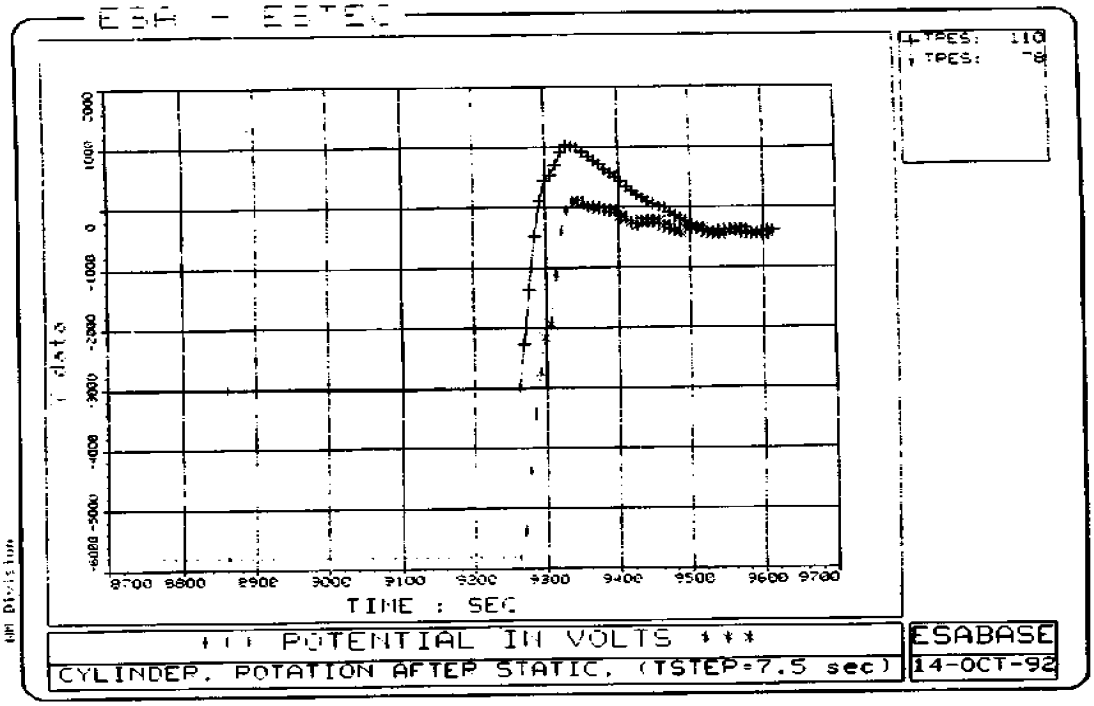

Fig.5a. NASCAP. Cylinder rotation after static charging. Start position of cell 110 is in center of illuminated surface, cell 78 - at 90^o relative to Sun direction.

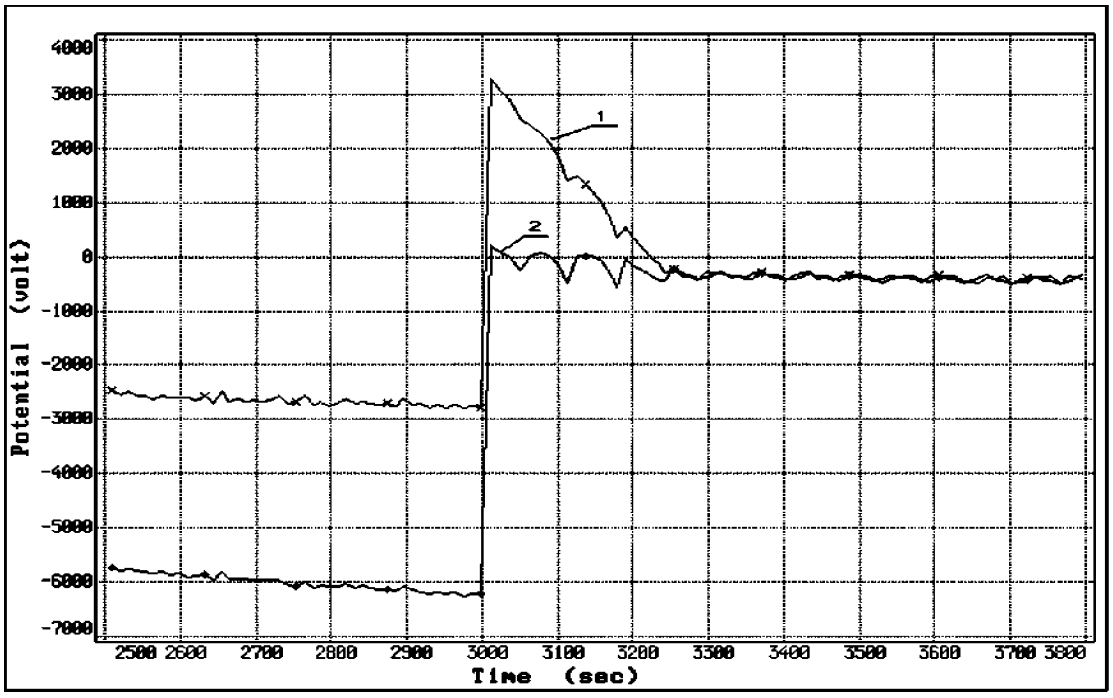

Fig.5b. ECO-M. Cylinder rotation after static charging (50 min after substorm begining). 1 - cell 110, 2 - cell 78.

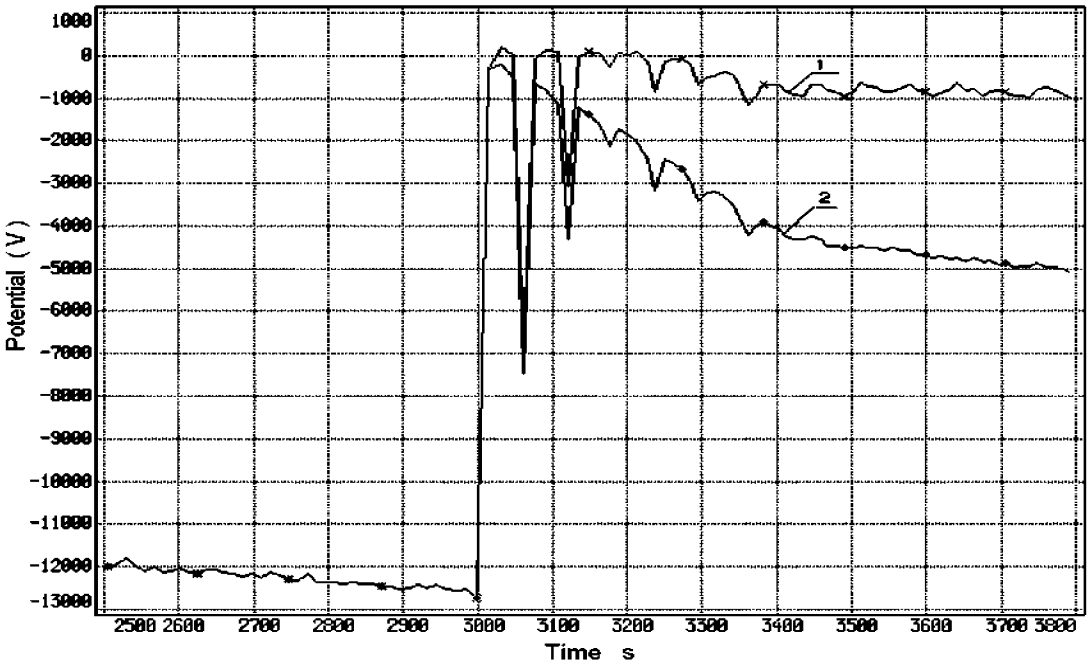

Fig.6a. ECO-M. Cylinder rotation after static charging (50 min after substorm beginning. 1 - cell 23, 2 - cell 61. Factor SEE σ_{total}=0.75.

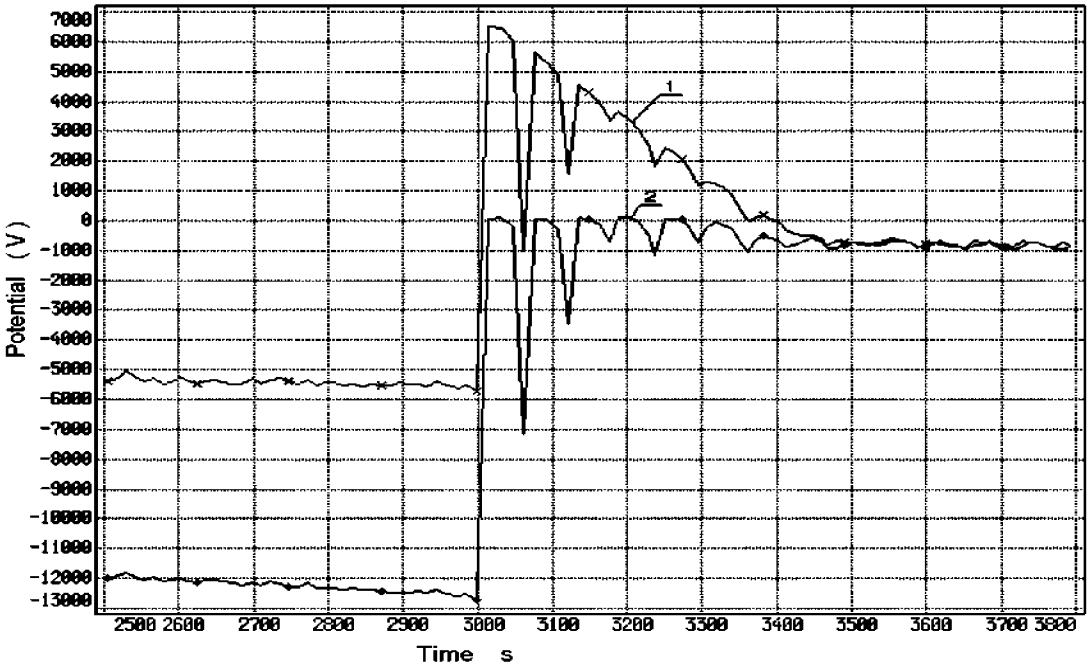

Fig.6b. ECO-M. Cylinder rotation after static charging (50 min after substorm beginning). 1 - cell 110, 2 -cell 78. Factor SEE σ_{total}=0.75.